Websites:
http://www.jofamericanscience.org
http://www.sciencepub.net

Emails:
editor@sciencepub.net
sciencepub@gmail.com

MARSLAND PRESS
Multidisciplinary Academic Journal Publisher

Amniotic Fluid Stem Cells Transplantation Generates Oocytes in Rat Model of Cyclophosphamide-Induced Premature Ovarian Failure. Histological and Immunohistochemical Study

Mohamed M. Saleh, Amany M. El Shawarby, Manal S. Hafez and Hany K. Mostafa

Histology Department, Faculty of Medicine, Ain Shams University, Cairo, Egypt
mohammedsanyor@gmail.com

Abstract: Introduction: Early menopause occurs in female cancer patient after chemotherapy. Amniotic fluid stem cells transplantation has been linked to the return of ovarian function. **Aim of work:** Was to investigate whether intravenously delivered human amniotic fluid stem cells (HAFSCs) could restore the structure and function of ovaries in a model of premature ovarian failure (POF) in rat. **Material and methods:** Forty five adult albino rats weighting 300-350 grams were used in this study. The animals were divided into the following groups group I (control group), group II this group was divided into 2 subgroups in which the animals received single intraperitoneal injection of 70 mg/kg cyclophosphamide, the animals were sacrificed after one week (subgroup IIA), and after two weeks (subgroup IIB). In group III the rats received the same dose of cyclophosphamide and one week later they received single dose of HAFSCs, two weeks later the animals were sacrificed. The ovaries were processed for histological and immunohistochemical study. Moreover, hormonal assay, morphometric and statistical study were done. **Results:** In subgroup IIA significant increase in the number of ovarian cysts was detected while the number of growing follicle and corpora lutea showed significant decrease. In subgroup IIB nearly all ovarian follicles were atretic with absence of corpora lutea. Sever inflammatory cellular infiltration of ovarian parenchyma with ovarian fibrosis could be seen. These results were associated with significant decrease in estradiol level compared to group I & III. Ovarian surface epithelium of this group revealed negative immunoreaction for CD105. In group III the ovaries regained their normal histological structure with presence of growing follicles, mature Graafian follicle and recent corpus luteum. These results were associated with positive CD105 immunoreactivity in ovarian surface epithelium (OSE), epithelial cyst and interstitium with significant increase in estradiol level**. Conclusion**: Human amniotic fluid mesenchymal stem cells injection (HAFSCs) could improve ovarian damage induced by cyclophosphamide treatment in rats. They could create good microenvironment for transformation of reserve stem cells into ovarian follicles.

[Mohamed M. Saleh, Amany M. El Shawarby, Manal S. Hafez and Hany K. Mostaf. **Amniotic Fluid Stem Cells Transplantation Generates Oocytes in Rat Model of Cyclophosphamide-Induced Premature Ovarian Failure. Histological and Immunohistochemical Study.** *J Am Sci* 2019;15(7):48-60]. ISSN 1545-1003 (print); ISSN 2375-7264 (online). http://www.jofamericanscience.org. 6. doi:10.7537/marsjas150719.06.

Keywords: Premature ovarian failure, Cyclophosphamide, Human amniotic fluid stem cells.

1. Introduction

Chemotherapy regimen caused reproductive damage in young female. The long term adverse effect of chemotherapy treatment was premature ovarian failure (POF) **(Tsiligiannis et al., 2019).**

Hou et al. (2013) reported that hormonal replacement therapy could alleviate estrogen deficiencies. However this therapy had been shown to increase breast cancer.

Stem cell therapy had been supposed as an alternative therapeutic measure.

Ghadami et al. (2012) reported that bone marrow mesenchymal stem cells (BMMSCs) could restore ovarian function and generate immature oocyte in female mice. **Abd-AllAh et al. (2013)** demonstrated that BMMSCS could contribute in recovering of ovarian structure and function that were injured by cyclophosphamide. **Hou et al. (2013)** investigated therapeutic potential of HAFMSCs in chemotherapy induced ovarian damage.

However the role of MSCs in cyclophosphamide treated ovary was not clear. Therefore the purpose of the present study was to evaluate the effect of intravenous injection of AFSCs on cyclophosphamide treated rat ovary.

2. Materials and Methods

Materials:

(A) Drugs:

1- Cyclophosphamide:

It was obtained in the form of powder vial 1 gram and purchased from Baxter pharmaceutical company. It prepared by dissolving the powder in 100 ml normal saline 0.9%. The rats received single intraperitoneal injection of70 mg/kg cyclophosphamide **(Liu et al., 2012).**

2- Preparation of human amniotic fluid mesenchymal stem cells (HAFSCs)

The technique was performed in the clinical pathology department faculty of medicine Ain Shames University.

Methods of amniotic fluid collection, separation and purification: (Spitzhorn et al., 2017)

1. Amniotic fluid collection

The amniotic fluid was collected from the amniotic sac during cesarean sections using sterile 50 ml vacuum syringe. Amniotic fluid was freshly transferred to the lab within 1 hour of collection in cooled ice.

2. Amniotic fluid stem cells separation

A. Amniotic fluid was filtered using specific vacuums for filtration of cells and purification from other debris.

B. The filtered amniotic fluid was transferred to 15 ml falcon tubes and centrifuged at 1200 rpm for 20min.

C. The supernatant was discarded and the cells pellet was washed 3 times by phosphate buffer saline PH7.4.

D. The cells pellet was re- suspended in 1 ml phosphate buffer saline PH7.4.

3. Amniotic fluid stem cells Isolation

Purified amniotic fluid stem cells were isolated using specific magnetic separation technique using magnetic beads (Human anti-TRA- 60microbeads; Miltenyi Biotec cat no: 130-100-832) so the separated cells are highly specific and pure.

Preservation

The isolated purified cells were preserved at -80 degree after addition of DEMSO 1%.1ml of human amniotic fluid stem cells (HAFSCs) -approximately $1x10^3$ cells /µl- were injected via the tail vein 1 week after administration of cyclophosphamide. Then the animals were sacrificed two week later **(Johnson et al., 2005).**

(B)Animals:

Forty five adult albino rats 300-350 grams in weight, between 4-5 weeks of age were used in this study. All rats were (3 - 4 / cage) maintained in a temperature controlled room under standard light-dark cycle. They had free access to food and water. The animals were divided into the following groups.

- **Group I (control group):**

Fifteen rats received balanced diet and were divided into 3 groups 5 animals each:

Group 1A: the rats received single intraperitoneal injection of 1 ml physiological saline.

Group 1B: the rats were injected with 1 ml of physiological saline in the tail vein.

Group 1C: the rats left untreated.

Group II (cyclophosphamide treated group):

This group was divided into 2 subgroups 10 animals each:

Subgroup IIA

Ten rats received single intraperitoneal injection of 70 mg/kg cyclophosphamide. One week later the animals were sacrificed **(Liu et al., 2012).**

Subgroup IIB

Ten rats received single intraperitoneal injection of 70 mg/kg cyclophosphamide; two week later animals were sacrificed.

Group III (stem cell treated group):

Ten rats received single intraperitoneal injection of 70 mg/kg Cyclophosphamide, and then the animals were injected with 1ml of HAFSCs (approximately $1x10^3$ cells/µl) via the tail vein 1 week after administration of cyclophosphamide. Then the animals were sacrificed two week later **(Johnson et al., 2005).**

Methods:

At the end of the experimental periods, blood samples were withdrawn from the tail vein then the animals were sacrificed by cervical dislocation under anesthesia by pentobarbital sodium. Their ovaries were dissected out and processed for the following:

1. Histological study.
2. Immunohistochemical study.
3. Hormonal assay.
4. Morphometric and Statistical Studies.

I. Histological study:

Sections stained using the following stains:-

1. Haematoxyline and eosin stain **(Bancroft & Gamble,2018).**

2. Modified Masson's Trichrome stain **(Bancroft & Gamble, 2018).**

II. Immunohistochemical study:

Some paraffin sections from each group were subjected to Immunohistochemical staining for caspase-3 and CD105 using the Avidin–Biotin–Peroxidase complex technique.

CD105 is also known as Endoglin. It is a type I integral membrane homodimer protein with subunits of 90 kD. It acts as a marker for human amniotic fluid mesenchymal stem cells **(Hamid et al., 2017).**

III. *Hormonal assay study:* Raju et al. (2013)

Estradiol and FSH values were measured in the blood of each group:

- 2 ml blood sample was collected from tail vein in 2 separate tubes.
- The samples were centrifuged for ten minutes at 4000RPM.
- Estradiol and FSH were measured by fluorescent immunoassay (VIDAS-Bio Merieux).

IV. Morphometric Study:

It was done for all group using image analysierleica Q win and Q go program in Histology department Faculty of Medicine Ain Shams University.

1. The mean number of primordial follicles, growing follicles, Graafian follicles, atretic ovarian follicles and recent corpus luteum were calculated.

2. The mean area percentage of collagen deposition.

These parameters were measured in 5 non overlapping fields from 5 different sections in each groups and subgroups using LPFx 100 HPFx400.

Statistical analysis:

Morphometric measured parameters and the values of hormonal assay recorded for each group were revised and the results were expressed as mean ± SD. Statistical analysis was carried out using statistical package for the social sciences (SPSS), software program, version 20 (IBM corporation, Armwork, North castle, Westchesten Country, New York, USA).

Statistical difference among groups for each parameter was determined using two way analysis of variance (ANOVA) followed by post hoc least significance difference (LSD) for comparison between more than two groups P value ≤ 0.05 were considered statistically significant.

Histological Results

Group I (Control group)

Light microscopic results:

The **H & E-stained** sections showed outer cortex of the ovary containing large recently formed corpora lutea with blood clots in their lumina. The surface of the ovary also contained cystic follicles and epithelial clefts. Many lobules of interstitial glands could be seen **(Fig 1**).

By higher magnification, the ovarian cortex showed different stages of ovarian development and large cystic follicle. The medulla showed blood vessels and interstitial glands **(Fig 2)**.

Surface of the ovary showed many corpora lutea projecting from the surface. Also cystic follicle and multilamellar follicle could be seen. Large interstitial glands and deep cleft were prominent in **(Fig 3)**

Surface epithelium showed sloughing of its cells. Some cells of surface epithelium underwent mesenchymal transformation. Old corpusluteum consisting of small vacuolated cells invaded with connective tissue septa while recent corpus luteum consisting of large acidophilic cells. **(Fig 4)**

Masson's trichrom stained section showed thin strands of collagen fibers around the congested blood vessels. Theca externa and zonapellucida were positively stained **(Fig 5)**

Immunohistochemical study revealed strongly positive immunoreactions for **CD 105** at the ovarian surface epithelium and cells of ovarian cysts **(Fig** 6).

Immunohistochemical study showed mild immunoreactions for caspase enzyme at granulosa cells of atretic ovarian follicle and cells of corpus luteum **(Fig 7).**

Group IIA

Connection between ovarian parenchyma and mesovarian was detected. The majority of the follicles were either atretic or cystic with deep epithelial clefts **(Figs 8,9).**

Cortex of the ovary showed many inclusion cysts that appeared migrating within stroma. Inflammatory cells and interstitial gland were prominent in the stroma **(Figs 10 and 11).**

Masson's trichrome stained sections showed prominent collagen fibers invading corpus luteum, follicular cysts and interstitium **(Fig 12).**

Immunohistochemical study revealed negative immunoreactions for **CD 105** at the ovarian surface epithelium **(Fig 13)**.

Immunohistochemical study using caspaseimmunostain revealed moderate immunoreactions at the atretic follicles, ovarian cysts and corpus luteum cysts **(Fig 14).**

Group IIB

The ovarian cortex in some specimen of this group revealed, inclusion cysts, many atretic follicles old corpus leutum Cellular infiltration of the parenchyma with prominent connective tissue septa were detected **(Fig 15)**.

The medulla of the ovary showed numerous thick- walled arterioles and thin dilated congested capillaries. Numerous atretic follicles, hemorrghic cysts and prominent interstitial glands could be seen. Cystic dilatations of reteovarii at the hilum of the ovary with excessive mesenchymal tissue infiltration were seen **(Figs 16,17).**

Masson's trichrome staining showed collagen fibers around blood vessels and around remnants of atretic follicles. Collagen fibers formed septa in between prominent interstitial glands **(Fig 18)**.

Immunohistochemical study revealed strong immunoreactions for caspase enzyme at the ovarian surface epithelium, atretic follicles, ovarian cysts, reteovarii cysts and corpus luteum cells **(Fig 19).**

Group III

In some specimen H & E stained sections revealed highly atrophied ovarian parenchyma with localized proliferation of stromal cells at the surface of the ovary. Multiple primordial follicles and growing follicles could be seen within proliferated stromal cells. Prominent interstitial gland could be detected **(Figs 20,21).**

Another specimen showed slightly atrophied ovary with growing follicles, recently formed corpus luteum, cystic follicles and cystic dilatation of reteovarii **(Fig 22).**

Another specimen showed more or less normal histological structure of the ovary **(Figs 23).**

In Masson trichrom stained sections thin strand of collagen fibers in theca externa of the

growing follicles and around blood vessels in the medulla could be seen **(Fig 24).**

Immunohistochemical study revealed positive immunoreactions for **CD 105** at the ovarian surface epithelium and ovarian cyst and interstitium **(Fig 25)**.

Immunohistochemical study revealed mild immunoreactions for caspase at the granulosa cells of atretic ovarian follicles, ovarian cysts and corpus luteum cells **(Fig 26).**

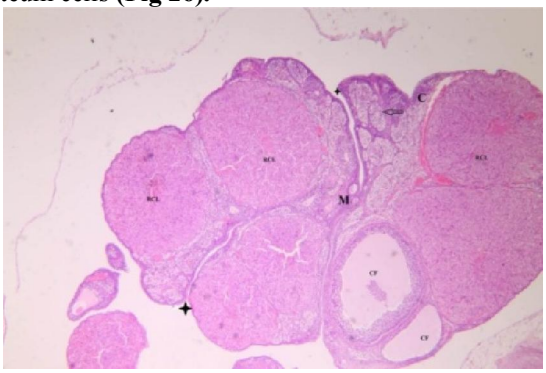

Fig. (1): Photomicrograph of section of the ovary (group I) showing outer cortex (**C**) and inner medulla **(M).** The surface is irregular with deeply in vaginated epithelial clefts (*) Cortex shows cystic follicles **(CF)**, recently formed corpora lutea **(RCL)** and interstitial glands **(←). (H & Ex40)**

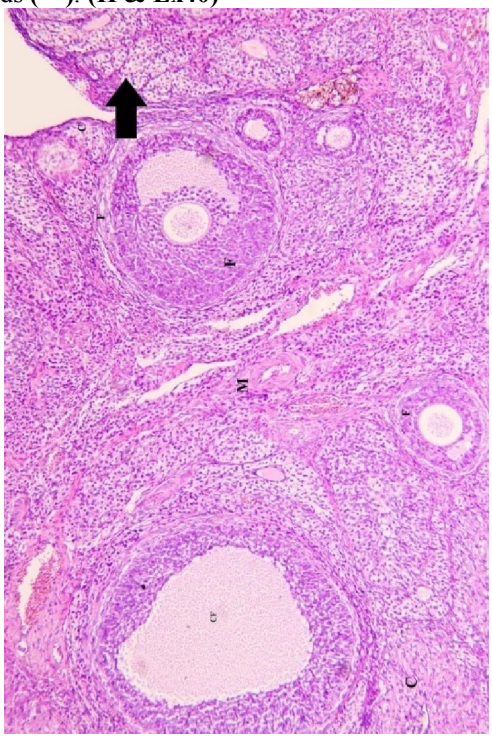

Fig. (2): Photomicrograph of section of the ovary (group I) showing outer cortex (**C**) and inner medulla **(M**). The cortex shows many follicles **(F)** in different stages of development and cystic follicle **(CF)**.Notice the presence of interstitial glands (↑). **(H & Ex100).**

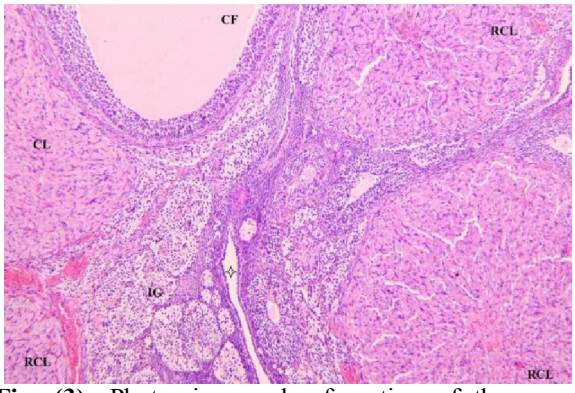

Fig. (3): Photomicrograph of section of the ovary (group I) showing large cyst (**CF**) lined by several layers of granulosa cells. It contains clear watery fluid. Recently formed corpora lutea **(RCL)** with blood in their lumen can be seen. The interstitium of the ovary contains interstitial glands **(IG)** and congested blood vessels. Notice the presence of epithelial clefts (*). **(H & Ex100).**

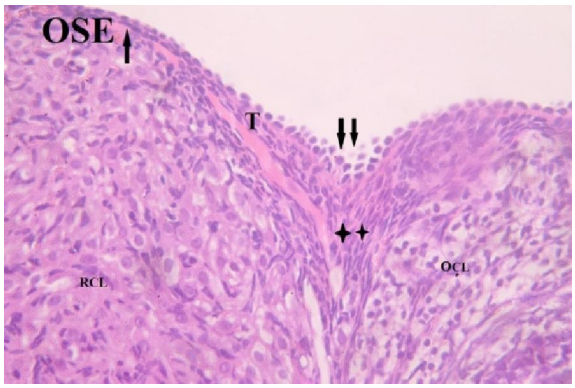

Fig. (4): Photomicrograph of section of the ovary (group I) showing surface epithelium of the ovary consisting of areas of flat cells **(OSE↑)** and exfoliated cells **(↓↓)**. Some surface epithelial cells undergo proliferation (**). Other cells transform into spindle shaped cells Notice old corpus luteum with small vacuolar degeneration of its cells and invasion by stromal cells (**OCL**). Recent corpus luteum with large acidophilic slightly vacuolated cells could be seen **(RCL) (H & Ex400).**

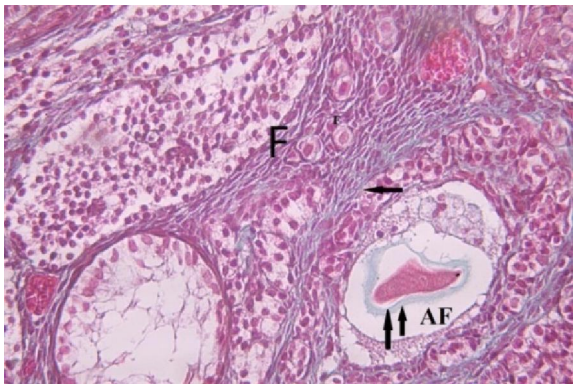

Fig. (5): Photomicrograph of section of the ovary (group I) showing collagen fibers around stromal cells and congested blood vessels in the interstitium of the ovary (←). Notice the presence of primordial follicles (**F**) and positively stained distorted zonapellucida (↑↑) of atretic follicle (**AF**). **(Masson's trichrome x400).**

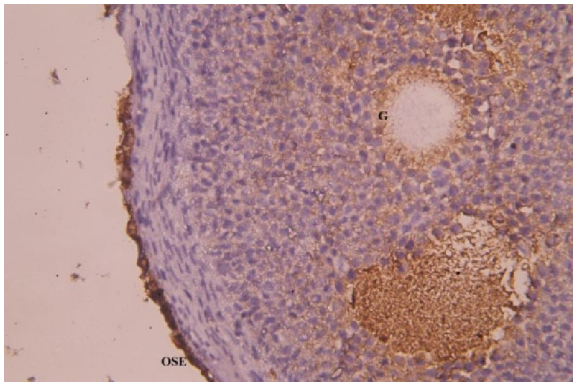

Fig. (6): Photomicrograph of section of the ovary (group I) showing positive immunoreactions for CD105 at the ovarian surface epithelium **(OSE)** and granulosa cells **(G)** of ovarian follicles. (CD105 immunostain x100).

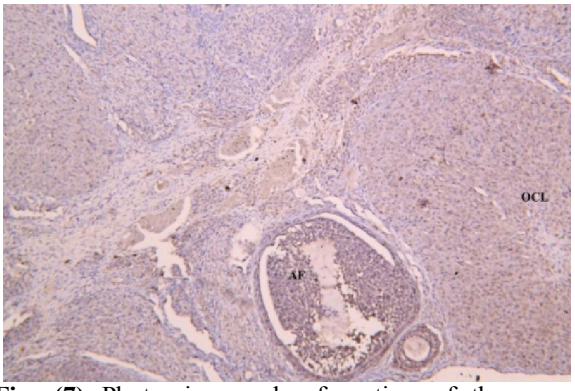

Fig. (7) Photomicrograph of section of the ovary (group I) showing mild immunoreactions for caspase enzyme of the atretic ovarian follicles **(AF)** and cells of old corpus luteum **(OCL). (Caspase-3 immunostainx100)**

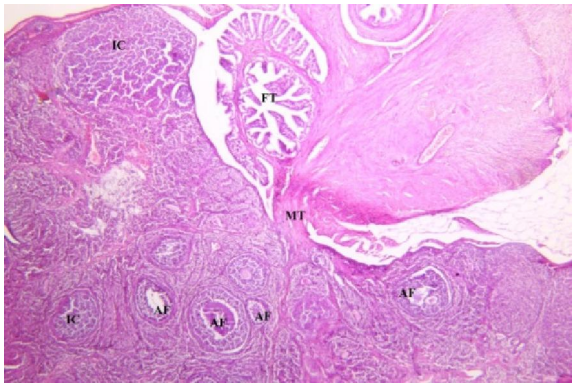

Fig. (8): A photomicrograph of section in the rat ovary group (IIA) showing part of ovarian parenchyma connected with mesovaroian tissue **(MT)** and part of fallopian tube **(FT).** The cortex of the ovary shows many atretic follicles (**AF**), inclusion cyst (**IC**). **(H & Ex100).**

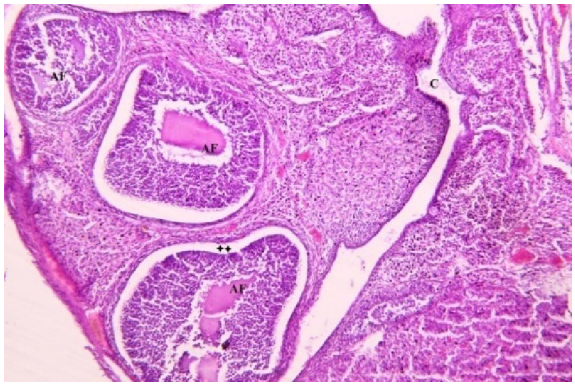

Fig. (9): A photomicrograph of section in the rat ovary group (IIA) showing deep epithelial cleft **(C)**, and many large atretic follicles (**AF)** with degenerated oocytes beneath blood vessels. Notice detachment of granulose cells from the basal lamina. (**) **(H & Ex400).**

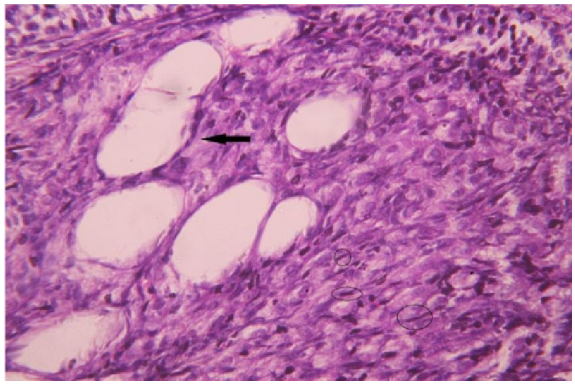

Fig. (10): A photomicrograph of section in the rat ovary group (IIA) showing multiple inclusion cysts (←). Notice the presence of dense spindle shaped migratory cells invading ovarian parenchyma in addition to inflammatory cells (○). **(H & Ex400).**

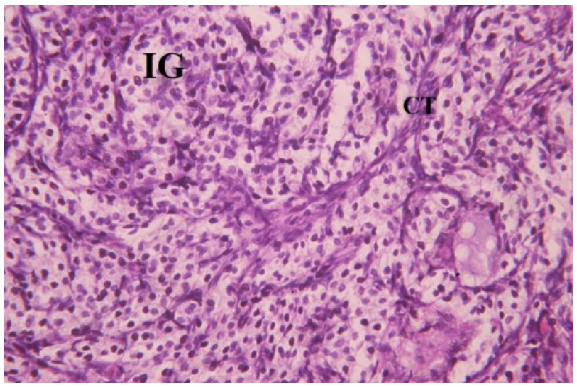

Fig. (11): A photomicrograph of section in the rat ovary group (IIA) showing interstitial glands of the ovary **(IG)** separated by connective tissue septa (CT) with heavy cellular inflammatory infiltration. **(H & Ex400).**

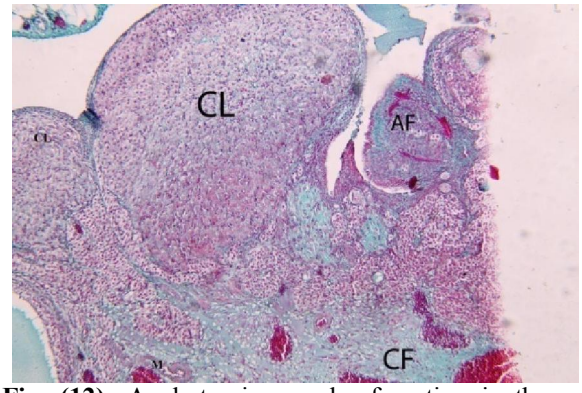

Fig. (12): A photomicrograph of section in the rat ovary group (IIA) showing dense collagen fibers (**CF**) in ovarian medulla. Notice invasion of collagen fibers into atretic follicle (**AF**) and corpora lutea (**CL**). **(Masson's trichrome x100).**

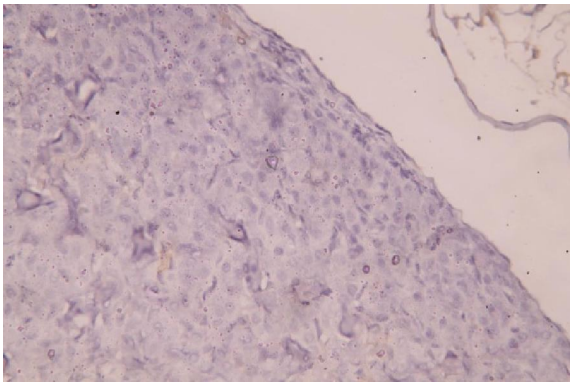

Fig. (13) A photomicrograph of section in the rat ovary group (IIA) showing negative immunoreactions for CD105 of the ovarian surface epithelium. (CD105 immunostainx100).

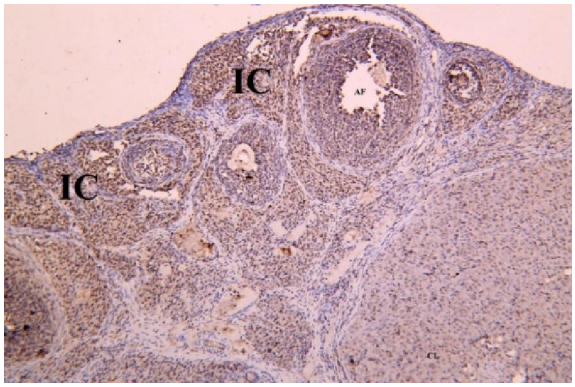

Fig. (14) A photomicrograph of section in the rat ovary group (IIA) showing moderate immunoreactions for caspase enzyme at the surface epithelium atretic follicles (AF) ovarian inclusion cyst, (IC) and corpus luteum cells (CL). (Caspase-3 immunostain x100).

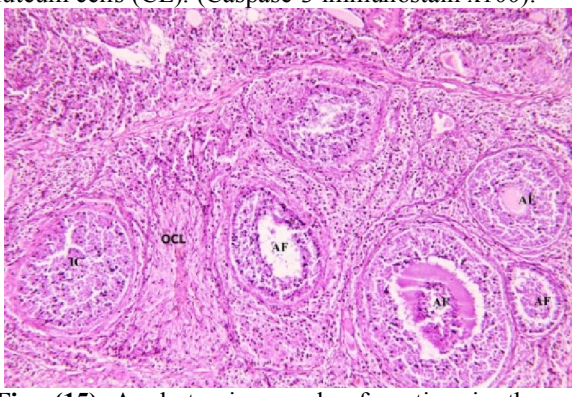

Fig. (15) A photomicrograph of section in the rat ovarian cortex group (IIB) showing, inclusion cyst (IC) and multiple large atretic ovarian follicles (AF), with degenerated oocytes and disrupted granulosa cells. Heavy cellular infiltration of ovarian parenchyma is prominent. Notice thick fibrous connective tissue septa and old corpus luteum (OCL). **(H & Ex100).**

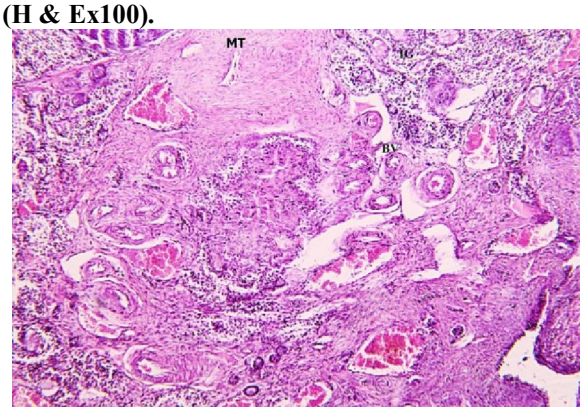

Fig. (16): A photomicrograph of section in the rat ovary group (IIB) showing medulla of the ovary consisting of numerous thick walled arterioles (BV), dilated congested capillaries, interstitial glands (IG) and thick mesovarian tissue (MT). **(H & E x100).**

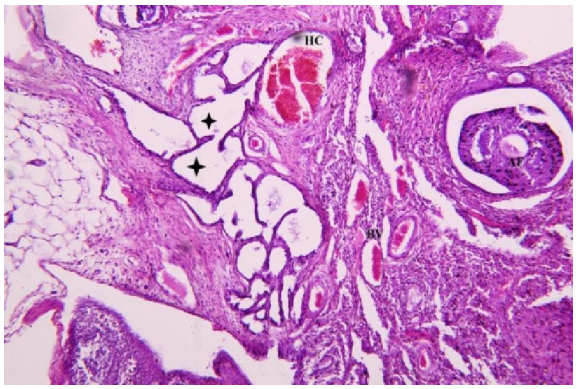

Fig. (17): A photomicrograph of section at the hilum of rat ovary group (IIB) showing cystic dilatation of rete ovarii (*), hemorrhagic cyst (HC) and atretic follicle (AF). **(H & Ex100).**

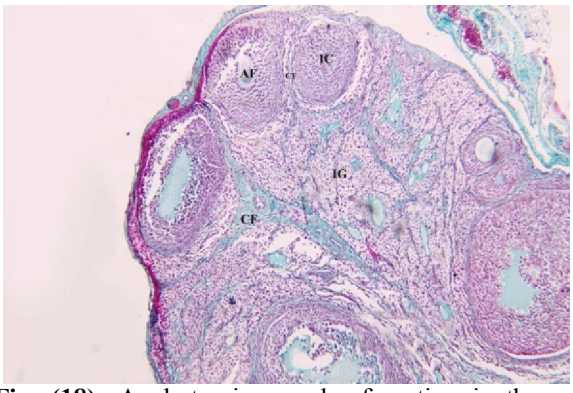

Fig. (18): A photomicrograph of section in the rat ovary group (IIB) showing strands of collagen fibers (CF) separating prominent interstitial glands (IG). Collagen fibers also surrounded remnants of atretic follicles (AF). **(Masson's trichrome x100)**

Fig. (19): Fig. (44): A photomicrograph of section of rat ovary group (IIB) showing strong immunoreactions for caspase in the granulosa cells of cystic ovarian follicles (CF), inclusion cysts (IC) and corpora lutea cells (CL). **(Caspase-3 immunostainx100)**

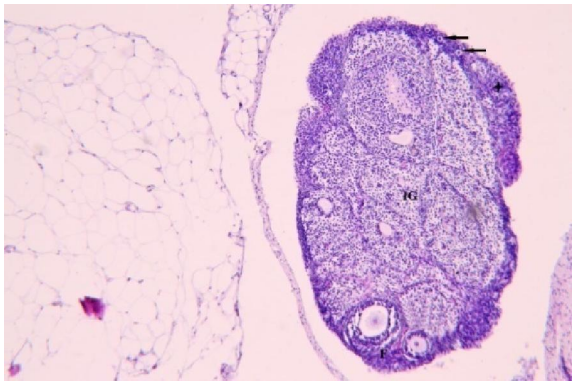

Fig. (20): A photomicrograph of section of rat ovary group (III) showing small sized ovary with localized aggregation of stromal proliferation at the surface (*). Many primordial follicles (←) and growing follicles **(F)** are detected. Notice that parenchyma of the ovary is formed mainly of prominent interstitial glands **(IG)**. **(H & Ex40).**

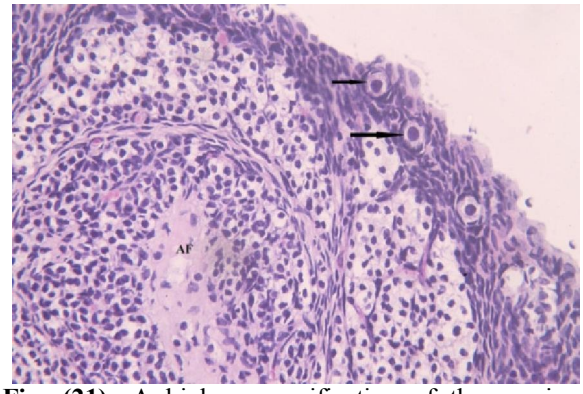

Fig. (21): A higher magnification of the previous section showing many primordial follicles within proliferating stromal cells at the surface of the ovary (←). Notice large atretic follicle (AF) with hyaline material inside its lumen. **(H & Ex400).**

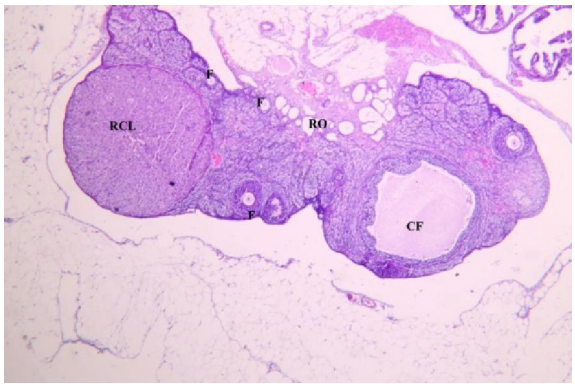

Fig. (22): A photomicrograph of section of rat ovary group (III) showing growing follicles (F), recently formed corpus luteum (RCL) and large cystic follicle (CF). Notice the presence of cystic dilatation of rete ovarii at the hilum (RO). **(H & Ex40).**

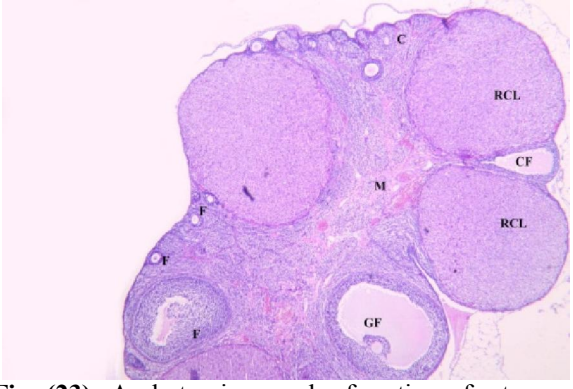

Fig. (23): A photomicrograph of section of rat ovary group (III) showing more or less normal ovarian structure. The outer cortex (C) contains primary follicles (F), mature Graafian follicle (GF), cystic follicle (CF) and recently formed corpora lutea (RCL). Inner medulla (M) contains blood vessels. **(H & Ex100).**

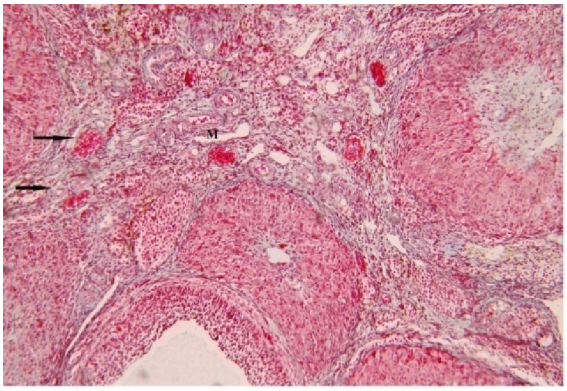

Fig. (24): A photomicrograph of a part of ovarian cortex group (III) showing collagen fibers around blood vessels (→) in the medulla (M) and around theca layers. **(Masson's trichrome x100).**

The Morphometric measurements and Statistical Results.

The mean area percentage of collagen:

There was a significant increase in the mean collagen area percentages of ovarian sections in both subgroup IIA and subgroup IIB as compared to the control rats. There was non-significant change in mean collagen area percentages of rats of group III as compared to control group. There was non-significant change in mean collagen area percentages of rats of both subgroups IIA and IIB as compared to each others, **(Table 1 and Histogram 1).**

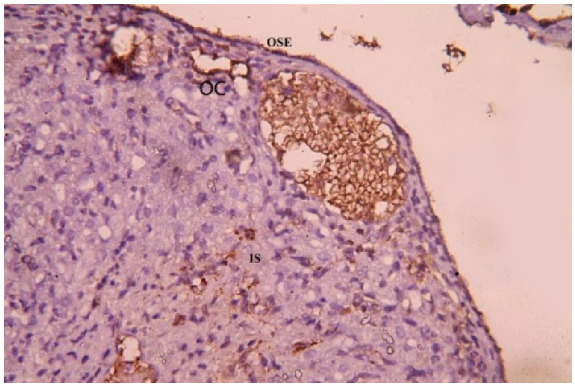

Fig. (25): A photomicrograph of section of rat ovary group (III) showing postive immunoreactions for CD105 of ovarian surface epithelium (OSE), ovarian cyst (OC) and interstitium (IS). (CD105 immunostainx100).

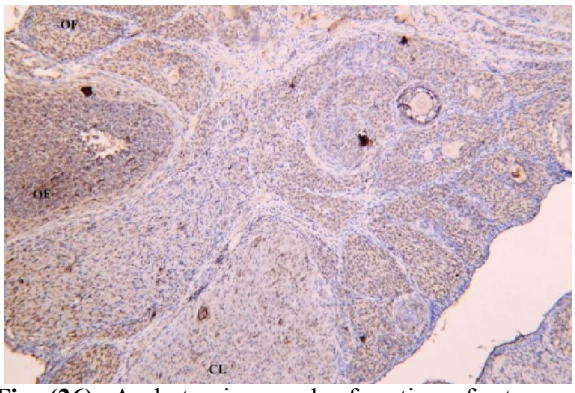

Fig. (26): A photomicrograph of section of rat ovary group (III) showing mild immunoreactions for at granulosa cells of large ovarian follicle (OF), ovarian cysts (OC), corpus luteum cells (CL). (Caspase -3 immunostainx100).

Table (1): The mean collagen area percentage in high power field images

	Mean ± SD	**P value**	**Significance**
Group I	3.61 ± 2.81		
subgroup IIA	20.44 ± 9.86	0.000	Significant increase
subgroup IIB	24.85 ± 10.65	0.000	Significant increase
Group III	5.4 ± 2.32	0.710	Non-Significant

*SD=3.61 ± 2.81*P value <0.05 significant P value >0.05 non significant

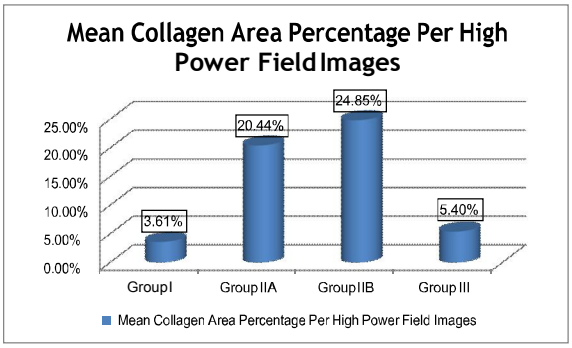

Histogram (1): Mean collagen area percentage per high power field images of different groups.

Mean number of Primordial Follicles:

Significant decrease in the mean number of primordial follicles of ovarian sections in both subgroup IIA and subgroup II B as compared to the control group. There was non significant differences between subgroup IIA and subgroup IIB. Non significant differences between group III and control group was observed **(Table 2 and Histogram 2).**

Table (2): The mean number of primordial follicles

	Mean ± SD	P value	Significance
Group I	1 ± 0.707		
subgroup IIA	zero	0.002	Significant decrease
Subgroup IIB	zero	0.002	Significant decrease
Group III	0.80 ± 0.447	0.461	Non-Significant

*SD=1 ± 0.707*P value <0.05 significant P value >0.05 non significant

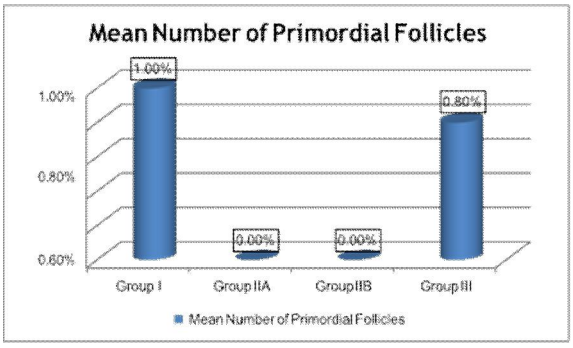

Histogram (2): Mean number of primordial follicles.

Mean number of Growing Follicles:

The measured data showed a significant decrease in the mean number of growing follicles of ovarian sections in both subgroups IIA and subgroup IIB as compared to the control group. Non-significant changes was observed in the mean number of growing follicles of group III as compared to the control group. Non significant change was observed between subgroup IIA and IIB, (**Table 3 and Histogram3).**

Table (3): The mean number of growing follicles

	Mean ± SD	P value	Significance
Group I	4.2 ± 1.09		
subgroup IIA	1.8 ± 0.83	0.011	Significant decrease
subgroup IIB	1.6 ± 0.54	0.006	Significant decrease
Group III	3.8 ± 2.16	0.637	Non-Significant

SD=4.2 ± 1.09P value <0.05 significant P value >0.05 non significant

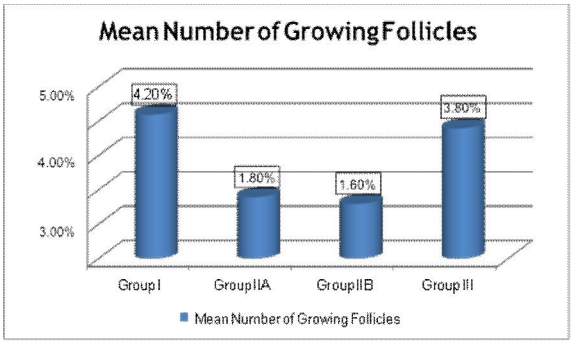

Histogram (3): Mean number of growing follicles.

Mean number of Graafian Follicles:

Significant decrease in the mean number of the mature Graafian follicles of ovarian sections in both subgroup IIA and group IIB as compared to the control group. Non-significant change was observed between group III and control group and in between group IIA and IIB, **(Table 4 and Histogram 4).**

Table (4): The mean number of Graafian follicles

	Mean ± SD	P value	Significance
Group I	0.6 ± 0.56		
subgroup IIA	zero	0.026	Significant
subgroup IIB	zero	0.026	Significant
Group III	0.5 ± 0.4	0.850	Non-Significant

*SD=0.6 ± 0.56*P value<0.05 significant P value>0.05= no significant

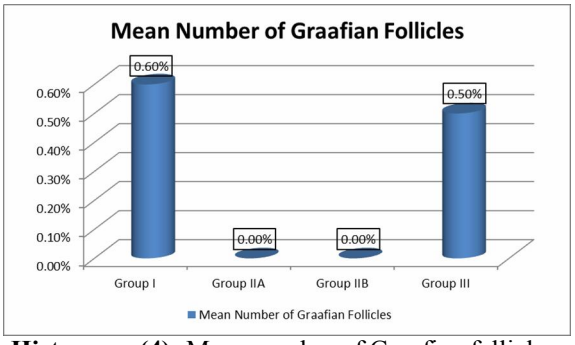

Histogram (4): Mean number of Graafian follicles.

Mean number of Atretic Follicles:

There was a significant increased in the mean number of atretic follicles of both subgroup IIA and subgroup IIB as compared to the control group. Non-significant changes were observed in the mean number of atretic follicles of group IIA as compared to the group IIB. Also non-significant changes were observed in the mean number of atretic follicles of group III as compared to the group I, (**Table 5 and Histogram5).**

Table (5): The mean number of atretic follicles

	Mean ± SD	P value	Significance
Group I	1.2 ± 0.44		
subgroup IIA	6.4 ± 1.14	0.000	Significant increase
subgroup IIB	6.2 ± 3.49	0.001	Significant increase
Group III	1 ± 0.3	0.790	Non-Significant

*SD=1.2 ± 0.44*P value<0.05 significant P value>0.05= no significant

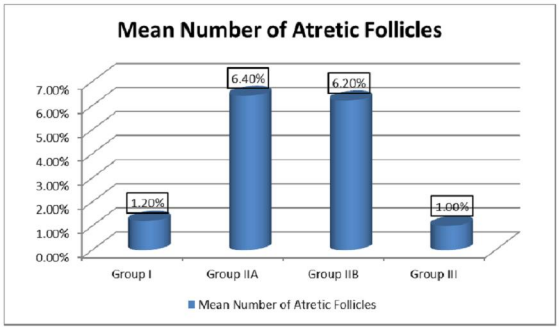

Histogram (5): Number of atretic follicles.

Mean number of recent Corpus Luteum:

There was a significant decrease in the mean number of recent corpus luteum of ovarian sections in both subgroup IIA and subgroup IIB as compared to the control group. Non-significant changes were observed in the mean number of recent corpus luteum of group IIA as compared to the group IIB. Also non-significant changes were observed in the mean number of recent corpus luteum of group III as compared to the group I, (**Table 6 and Histogram 6).**

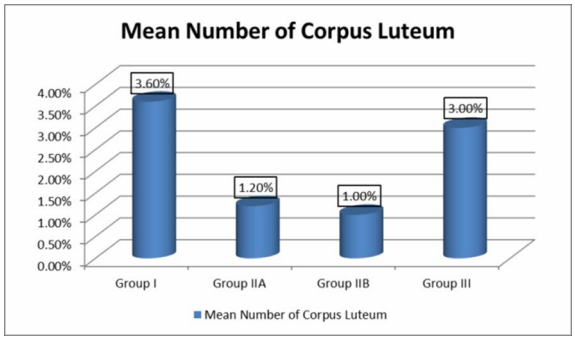

Histogram (6): mean number of corpus luteum.

Statistical Results of Hormonal levels

Mean serum level of follicular stimulating hormone (FSH):

Non significant difference in FSH level between all groups is observed (**Table 7 and Histogram 7).**

Table (6): The mean number of corpus luteum

	Mean ± SD	P value	Significance
Group I	3.6 ± 1.94		
subgroup IIA	1.2 ± 0.83	0.007	Significant decrease
subgroup IIB	1 ±.000	0.004	Significant decrease
Group III	3 ± 1.22	0.450	Non-Significant

SD=3.6 ± 1.94P value<non significant P value > significant

Table (7): The mean FSH levels

	Mean ± SD	P value	Significance
Group I	9.92 ± 1.65		
subgroup IIA	11.82 ± 1.63	0.145	Non-Significant
subgroup IIB	12.84 ± 1.8	0.339	Non-Significant
Group III	10.18 ± 0.9	0.710	Non-Significant

SD=9.92 ± 1.65P value<non significant P value > significant

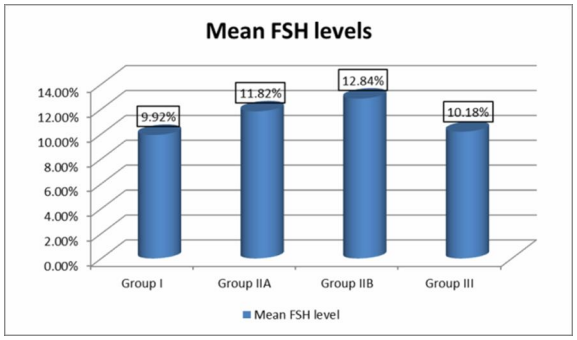

Histogram (7): Mean FSH levels

Mean serum level of estradiolhormone

Significant decrease of the mean values of estradiol hormone of subgroup IIA and subgroup IIB as compared to the control group. There was no significant difference of mean value of estradiol hormone of group III as compared to control group **(Table 8 and Histogram8).**

Table (8): The mean Estradiol levels

	Mean ± SD	P value	Significance
Group I	14.96 ± 3.7		
subgroup IIA	10.12 ± 2.91	0.091	Significant decrease
subgroup IIB	9.3 ± 2.11	0.281	Significant decrease
Group III	11.34 ± 1.81	0.461	Non-Significant

SD=14.96 ± 3.7P value<non significant P value > significant

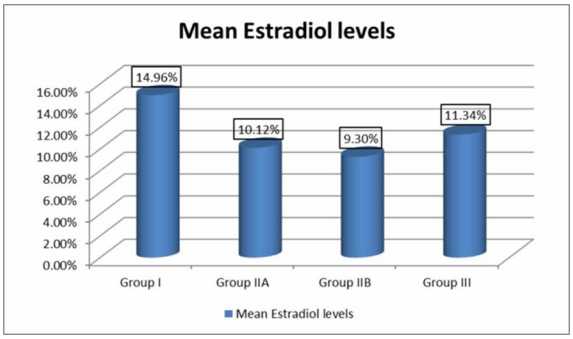

Histogram (8): Mean estradiol levels.

4. Discussion

Normally rat ovary contained few number of epithelial clefts and cysts **(Yen and Jaff, 2014)**. Moreover **Kumar et al. (2018)** stated that these crypts were originated from unrupturedgraafian follicles or incomplete atresia of the follicles.

In group II of the present study significant increase in the number of these cyst was recorded. **Acloque et al. (2009) and Gendronneau et al. (2012)** declared that these cysts could result from the failure of epithelial mesenchymal transition EMT. EMT is homeostatic mechanism that allowed incorporation of epithelial cells of the ovarian surface into ovarian stroma. Failure of EMT resulted in epithelial cell aggregation forming cysts.

In group II and III of the present study rete ovarii cysts were seen. Also, **Park et al. (2012)** recorded their presence in post menopausal women. Moreover, **Dubeau and Drabkin, (2013)** recorded the presence of stem cells in ovarian cysts.

Significant increase in atretic follicles number with significant decrease in corpora lute number was

recorded in the group II of the present study also follicular atresia was confirmed by increase caspase-3 immunoreactivity in group II. Moreover, **Zhao et al. (2010)** explained over apoptosis of granulosa cells in the cyclophosphamide treated group. They stated that cyclophosphamide treatment led to increase mitochondrial membrane permeability leading to cytochrome c release and activation of caspase 3 enzyme. Over apoptosis of granulosa cells resulted in significant decrease in estradiol level in group II. On the other hand FSH showed no significant differences between all groups. Also (Justin et al 2018) stated that cyclophosphamide induced change in receptor and molecular form in FSH resulting in the development of FSH insensitivity. Also, over apoptosis of granulosa cells led to decrease expression of anti mullerian factor (AMF1). AMF1 is produced by granulosa cells of ovarian follicles and control the rate at which ovarian follicles become available for preovulatory development. Normally AMF1 can inhibit FSH release these resulted in over-activation of large number of follicles and exhaustion of follicular reserve **(Seifer and Merhi, 2014).**

Exhaustion of ovarian stem cells could explain the absence of CD 105 seen in the group II of the present study.

Excessive cellular infiltration and ovarian fibrosis could be seen in group II. **Marder et al. (2012)** declared that POF associated with cyclophosphamide was an autoimmune disease. In this disease activation oh T helper 1 led to release of gamma interferon and activation of macrophages. Macrophages produce TNF which Allowed apoptosis of granulosa cells and endothelial cells leading to ovarian atrophy and ischemia.

In the group III of the present study some ovarian specimen still showed absence of corpora lutea and formed of numerous interstitial glands. However proliferation of stromal cells occurred at ovarian surface which might originate from EMT of the OSE. These proliferated stromal cells contained primordial and small growing follicles. These results confirmed by positive immunoreaction for CD105. The other specimen showed normal ovarian structure.

Also, **Johnson et al. (2004)** recorded the presence of germ cells in OSE that were positive for alkaline phosphatase and zonapellucida protein (ZPP).

Celik et al. (2012) recorded that OSE contained very small embryonic like stem cells (VSELS). Moreover, **Kucia et al. (2013)** stated that although chemotherapy resulted in complete loss of ovarian reserve,

VSELS survived and underwent oocyte specific differentiation. However. **Findlay et al. (2015)** stated that at birth ovary contained maximum number of ovarian germ line. Germ line stem cells did not contribute new oocyte to ovarian reserve in adult ovary.

Group III of the present study showed significant increase in the number of growing follicles and corpora lutea with decrease in the atretic follicles number, cellular infiltration and fibrosis. These results were confirmed by decrease in caspase-3 immunoreaction and significant decrease in collagen fibers deposition.

Conclusion

Injection of AFSCs resulted in recovery of ovarian follicles and resumption of ovulation process in a model of POF induced by cyclophosphamide treatment in rats.

References

1. Abd-Allah SH, Shalaby SM, Pasha HF, El-Shal AS, Raafat N, Shabrawy SM, Awad HA, Amer MG, Gharib MA, El Gendy EA (2013): Mechanistic action of mesenchymal stem cell injection in the treatment of chemically induced ovarian failure in rabbits. Cytotherapy; 15:64–75.
2. Acloque H, Adams MS, Fishwick K, Bronner-Fraser M, Nieto MA (2009): Epithelial-mesenchymal transitions: the importance of changing cell state in development and disease. J. Clin. Invest; 119: 1438–1449.
3. Bancroft JD and Gamble M (2018): Theory and practice of histological Techniques: 10th edition. Churchill Livingstone, NY. 2007.
4. Celik O, Celik E, Turkcuoglu I, Yilmaz E, Simsek Y, Tiras B (2012): Germline cells in ovarian surface epithelium of mammalians: a promising notion. Reprod Biol Endocrinol; 10: 112.
5. Dubeau L and Drapkin R (2013): Coming into focus: the nonovarian origins of ovarian cancer. Ann Oncol; 24: viii28–viii35.
6. Findlay JK, Hutt KJ, Hickey M, Anderson RA (2015): How Is the Number of Primordial Follicles in the Ovarian Reserve Established? Biology of Reproduction; 93(5):1–7.
7. Gendronneau G, Boucherat O, Aubin J, Lemieux M, Jeannotte L (2012): The loss of Hoxa5 function causes estrous acyclicity and ovarian epithelila inclusion cysts. Endocrinology; 153: 1484–1497.
8. Ghadami M, El-Demerdash E, Zhang D, Salama SA, Binhazim AA, Archibong AE, Chen X, Ballard BR, Sairam MR, Al-Hendy A (2012): Bone marrow transplantation restores follicular maturation and steroid hormones production in a mouse model for primary ovarian failure. PLoS

One; 7(3): e32462.

9. Hamid AA, Joharry MK, Mun-Fun H, Hamzah SN, Rejali Z, Yazid MN, Karuppiah T and Nordin N (2017): Highly potent stem cells from full-term amniotic fluid: A realistic perspective. Journal: Reproductive Biology; 17(1):9-18.
10. Hou N, Hong S, Wang W, Olopade OI, Dignam JJ, Huo D (2013): Hormone Replacement Therapy and Breast Cancer: Heterogeneous Risks by Race, Weight, and Breast Density. JNCI Journal of the National Cancer Institute; 105(18): 1365-1372.
11. Johnson J, Bagley J, Skaznik-Wikiel M, Lee HJ, Adams GB, Niikura Y, et al. (2005): Oocyte generation in adult mammalian ovaries by putative germ cells in bone marrow and peripheral blood. Cell; 122: 303–315.
12. Johnson J, Canning J, Kaneko T, Pru JK, Tilly JL (2004): Germline stem cells and follicular renewal in the postnatal mammalian ovary. Nature; 11(428)145–150.
13. Kucia M, Masternak M, Liu R, Shin DM, Ratajczak J, Mierzejewska K, et al. (2013): The negative effect of prolonged somatotrophic/insulin signaling on an adult bone marrow-residing population of pluripotent very small embryonic-like stem cells (VSELs). Age (Dordr); 35: 315–330.
14. Kumar V, Abbas AK and Aster JC (2018): Robbin basic pathology 10th edition; Slseviep. Philadelphia2018.
15. Liu T, Huang Y, Guo L, Cheng W, Zou G (2012): CD44+/CD105+ Human Amniotic Fluid Mesenchymal Stem Cells Survive and Proliferate in the Ovary Long-Term in a Mouse Model of Chemotherapy-Induced Premature Ovarian Failure. International Journal of Medical Sciences; 9(7):592-602.
16. Marder W, Fisseha S, Ganser MA, Somers EC (2012): Ovarian Damage During chemotherapy in Autoimmune Diseases: Broad Health Implications beyond Fertility. Clin Med Insights Reprod Health; (6):9–18.
17. Park J, Kim TH, Lee HH, Lee W, Chung SH (2012): Ovarian Rete Cyst in a Post-menopausal Woman: A Case Report J Korean Soc Menopause; 18(1): 67-69.
18. Raju GA, Chavan R, Deenadayal M, et al. (2013): Luteinizing hormone and follicle stimulating hormonesynergy: Areviewofrole in controlled ovarian hyper-stimulation. J Hum Reprod Sci; 6(4): 227–234.
19. Seifer DB and Merhi Z (2014): Is AMH a regulator of follicular atresia? Journal of Assisted Reproduction and Genetics; 31(11):1403-1407.
20. Spitzhorn LS, Rahman MS, Schwindt L, et al. (2017): Isolation and Molecular Characterization of Amniotic Fluid-Derived Mesenchymal Stem Cells Obtained from Caesarean Sections. Stem Cells Int; 5932706.
21. Tsiligiannis S, Panay N, Stevenson JC (2019): Premature Ovarian Insufficiency and Long-Term Health Consequences. Curr Vasc Pharmacol; Epub 2019 Jan 21.
22. Yen & Jaffe (2014): Reproductive endocrinology. Australia: Elsevier Inc. pages from 157 and 191.
23. Zhao XI, Huang YH, Yu YC, Xin XY (2010): GnRH antagonist cetrorelix inhibits mitochondria-dependent apoptosis triggered by chemotherapy in granulose cells of rats. Gynecol Oncol. 2010; 118:69–75.

7/9/2019